

Stress-induced non-vesicular release of prothymosin- α initiated by an interaction with S100A13, and its blockade by caspase-3 cleavage

H Matsunaga^{1,2} and H Ueda^{*1}

The nuclear protein prothymosin- α (ProT α), which lacks a signal peptide sequence, is released from neurons and astrocytes on ischemic stress and exerts a unique form of neuroprotection through an anti-necrotic mechanism. Ischemic stress-induced ProT α release is initiated by a nuclear release, followed by extracellular release in a non-vesicular manner, in C6 glioma cells. These processes are caused by ATP loss and elevated Ca²⁺, respectively. S100A13, a Ca²⁺-binding protein, was identified to be a major protein co-released with ProT α in an immunoprecipitation assay. The Ca²⁺-dependent interaction between ProT α and S100A13 was found to require the C-terminal peptide sequences of both proteins. In C6 glioma cells expressing a Δ 88–98 mutant of S100A13, serum deprivation caused the release of S100A13 mutant, but not of ProT α . When cells were administered apoptogenic compounds, ProT α was cleaved by caspase-3 to generate a C-terminal peptide-deficient fragment, which lacks the nuclear localization signal (NLS). However, there was no extracellular release of ProT α . All these results suggest that necrosis-inducing stress induces an extracellular release of ProT α in a non-vesicular manner, whereas apoptosis-inducing stress does not, owing to the loss of its interaction with S100A13, a cargo molecule for extracellular release.

Cell Death and Differentiation (2010) 17, 1760–1772; doi:10.1038/cdd.2010.52; published online 14 May 2010

Prothymosin- α (ProT α), a nuclear protein, is widely distributed throughout the body and has various intracellular functions in determining life and death.^{1,2} ProT α bearing a conventional nuclear localization signal (NLS) is largely localized in the nucleus, and has important functions in the regulation of cell differentiation and proliferation.^{1–3} When a cell is subjected to apoptotic stimuli, on the other hand, ProT α is released from the nucleus to the cytosol in which it inhibits apoptosome formation.⁴ Thus, ProT α is supposed to have a proliferative function in the nucleus under normal conditions, and a self-defensive function in the cytosol under apoptotic conditions.

We have recently identified ProT α as a unique anti-neuronal necrosis factor in the conditioned medium (CM) of cortical neurons,⁵ and discovered its potent neuroprotective functions in cerebral and retinal ischemia.^{6,7} This protein is extracellularly released on starving or ischemic stress, and inhibits necrosis by inducing the membrane translocation of glucose transporters, which are endocytosed under ischemic conditions, resulting in an acceleration of necrosis owing to energy crisis.⁵ On the basis of pharmacological analyses, ProT α -induced translocation of glucose transporters is mediated by stimulation of a putative G_{i/o}-coupled receptor, phospholipase C, and protein kinase C (PKC) β_{11} . This fact indicates that ProT α has another self-defensive function as an extracellular signal under conditions inducing necrosis.

However, little is known of the mechanisms underlying extracellular ProT α release. Of importance are the facts that the majority of ProT α content in the nucleus is extracellularly released on stress, before membrane disruption,⁵ and that ProT α lacks a signal peptide sequence, which is required for sorting to the endoplasmic reticulum (ER)-Golgi system before exocytosis. Therefore, ProT α release seems to proceed in a non-classical or non-vesicular manner under ischemic stress conditions. Here, we report the ischemia-induced nuclear release of ProT α , followed by its interaction with S100A13, a cargo molecule for extracellular release. We also discuss the mechanism underlying the lack of extracellular ProT α release under apoptotic conditions.

Results

Serum-deprivation stress-induced non-classical release of ProT α . ProT α is exclusively localized in the nuclei of various cells, including neurons.^{1–3} Starvation stress caused by serum deprivation induced a disappearance of ProT α from neurons and astrocytes, as early as 3 h after the start of primary culture (Figure 1a). Recently, we discovered the release of this protein into the CM of cultured cortical neurons under serum-free starving conditions causing necrosis.⁵

¹Division of Molecular Pharmacology and Neuroscience, Department of Molecular Medicinal Sciences, Nagasaki University Graduate School of Biomedical Sciences, 1-14 Bunkyo-machi, Nagasaki 852-8521, Japan

*Corresponding author: H Ueda, Division of Molecular Pharmacology and Neuroscience, Department of Molecular Medicinal Sciences, Nagasaki University Graduate School of Biomedical Sciences, 1-14 Bunkyo-machi, Nagasaki 852-8521, Japan. Tel: +81 95 819 2421; Fax: +81 95 819 2420; E-mail: ueda@nagasaki-u.ac.jp

²Current address: Department of Applied Life Science, Faculty of Biotechnology and Life Science, Sojo University, Ikeda 4-22-1, Kumamoto 860-0082, Japan

Keywords: non-vesicular release; prothymosin- α ; S100A13; necrosis and apoptosis

Abbreviations: BDNF, brain-derived neurotrophic factor; BSA, bovine serum albumin; CM, conditioned medium; DAMPs, damage-associated molecular patterns; 2-DG, 2-deoxy-D-glucose; ER, endoplasmic reticulum; FGF, fibroblast growth factor; FRET, fluorescence resonance energy transfer; HMGB1, high-mobility group box1; NLS, nuclear localization signal; OU, oscillation unit; PKC, protein kinase C; ProT α , prothymosin- α ; QCM, quartz crystal microbalance

Received 06.8.09; revised 14.1.10; accepted 26.1.10; Edited by L Greene; published online 14.5.10

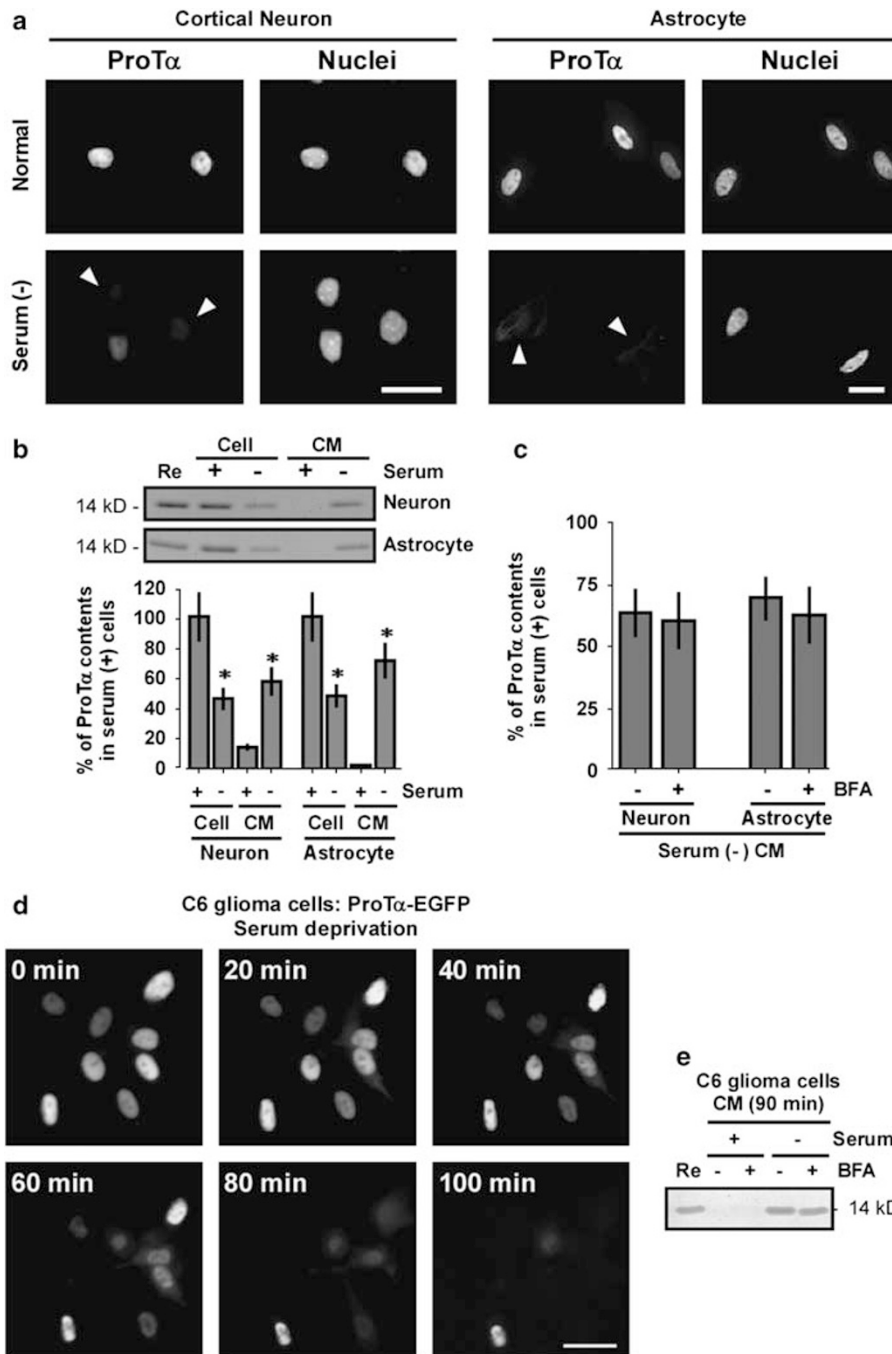


Figure 1 Serum-deprivation stress induced the brefeldin-A-insensitive non-classical extracellular release of ProT α . **(a)** Altered distribution of ProT α in cortical neurons and astrocytes. Cells were fixed for immunocytochemistry 3 h after serum-deprivation stress, indicated as serum (-). Arrowheads denote the nuclei of cells showing ProT α release. **(b)** ProT α release in cortical neurons and astrocytes induced by serum (-) stress. ProT α , a highly acidic protein, was purified from 5×10^5 cells and their CM using a phenol extraction procedure, and visualized with Coomassie brilliant blue. Data represent the means \pm S.E.M. of five independent experiments [$*P=0.01$, versus the corresponding serum (+) treatment]. **(c)** Characterization of brefeldin A-insensitive non-classical extracellular release of ProT α . Brefeldin A (BFA; $8 \mu\text{g/ml}$) was added to the culture of cortical neurons and astrocytes 12 h before serum deprivation. CM samples ($n=5$) were used for the purification of ProT α . **(d)** Real-time imaging of serum-deprivation stress-induced ProT α release. ProT α -EGFP stably expressed in C6 glioma cells was released on serum-deprivation stress. **(e)** Serum-deprivation stress-induced ProT α release in a BFA-insensitive manner. CM samples from C6 glioma cells culture were collected at 90 min after serum-deprivation stress (90 min). Scale bars represent $20 \mu\text{m}$. Re: recombinant rat ProT α

As shown in Figure 1b, when serum-derivation stress was given to neurons or astrocytes, the amounts of ProT α in both cell types markedly decreased at 3 h. On the other hand, the ProT α levels in the CM of both cell types in the presence of

serum were negligible. However, the serum-deprivation stress caused a significant extracellular release of ProT α from both cell types. Brefeldin A, a blocker of protein transport from the ER to the Golgi apparatus, did not affect

ProT α release (Figure 1c), suggesting that the manner of release differs from conventional vesicular release. Extracellular release of ProT α was also observed in a rat astroglial C6 glioma cell line after serum deprivation. In C6 glioma cells expressing ProT α -EGFP, the serum-deprivation stress-induced decrease of fluorescence in nuclei started as early as 20 min after serum deprivation, and complete disappearance was observed at 80 min, although a small population of cells (below 5%) still retained fluorescence (Figure 1d). However, no significant fluorescence signal was observed in the cytosol at these time points, suggesting that stress-induced nuclear export of ProT α is a rate-limiting step in the non-classical extracellular release of ProT α . As seen with primary neurons and astrocytes, brefeldin A did not affect the serum-deprivation stress-induced release of native ProT α release from C6 glioma cells (Figure 1e).

ATP-dependent nuclear localization of ProT α . We have earlier reported that serum-free starvation stress causes a rapid decrease in cellular ATP levels, leading to necrosis and extracellular ProT α release from the nucleus.⁵ As shown in Figure 2a, the addition of 2-deoxy-D-glucose (2-DG) to cultured C6 glioma cells in serum-containing medium caused a rapid decrease in ATP levels. When the subcellular localization of ProT α was examined (Figure 2b), the addition of 2-DG to cells without serum-starvation stress decreased the number of cells showing nuclear localization of ProT α , and increased the number showing cytosol localization. However, no significant extracellular ProT α release was observed. On the other hand, serum-deprivation treatment decreased the number of cells showing nuclear localization and increased the number showing extracellular release. Thus, these results suggest that the loss of cellular ATP induces the transport of ProT α from the nucleus to cytosol, but is not sufficient to cause extracellular release of ProT α from the cytosol.

We studied the machinery underlying nucleus-to-cytosol export. When Alexa Fluor488-labeled ProT α and Alexa Fluor568-bovine serum albumin (BSA) were co-injected into the cytosols of C6 glioma cells, Alexa Fluor488-ProT α was rapidly localized to the nucleus, within 10 min, whereas Alexa Fluor568-BSA remained in the cytosol (Figure 2c, upper left 4 panels). Treatment of cells with 2-DG abolished the nuclear localization of Alexa Fluor488-ProT α and redistributed it throughout the cell (Figure 2c, upper middle 4 panels). This re-distribution was completely reversed by co-injection of ATP (Figure 2c, upper right 4 panels). On the other hand, serum deprivation caused a re-distribution of ProT α from nucleus to cytosol, but did not result in extracellular release in the presence of amlexanox, which inhibits the release of proteins lacking a signal peptide sequence^{8–11} (Figure 2c, lower panels). Similarly, co-injection of ATP reversed the nucleus-to-cytosol export. Thus, it is evident that nuclear localization of ProT α is closely related to the cellular ATP level.

Importin α has an important function in the nuclear localization of proteins possessing an NLS. For the sustained localization of such proteins, importin α should be released into the cytosol for repeated use. The GTP-bound form of Ran, a small GTP-binding protein, is known to execute this importin recycling process.¹² Therefore, the loss of cellular

ATP is expected to impair the nuclear localization of ProT α owing to difficulty maintaining the GTP-bound state of Ran. Indeed, the nuclear localization of ProT α -EGFP was clearly impaired by injection of anti-importin α IgG into C6 glioma cells (Figure 2d). However, the nuclear levels of ProT α were not affected by leptomycin B, an inhibitor of the nuclear export receptor CRM1 (data not shown). When wheat germ agglutinin, an inhibitor of the nuclear pore complex, was injected into the nuclei of C6 glioma cells, ProT α was redistributed throughout the cells (Figure 2e). All of these findings suggest that ProT α is localized in the nucleus through an ATP-dependent importin-NLS mechanism,¹³ and that nucleus-to-cytosol export owing to loss of ATP occurs through passive diffusion.

Stress-induced extracellular co-release of ProT α with S100A13. When the CM from serum-deprived C6 glioma cells was immunoprecipitated with anti-ProT α IgG, two significant protein bands were stained by CBB (Figure 3a). The upper band was identified as ProT α by immunoblot using an acidic protein transfer procedure.¹⁴ The lower band, at approximately 10 kDa, was identified by matrix-assisted laser desorption/ionization-time of flight (MALDI-TOF) (five peptides, 57.1% coverage) followed by MS/MS sequence-tag analysis using the NCBI protein database, as S100A13, a member of the Ca²⁺-binding S100 family.^{15–17} Immunoblotting also confirmed that this protein is identical to S100A13.

As shown in Figure 3b, naturally occurring ProT α is localized within nuclei, whereas S100A13 is evenly distributed throughout cells. When cultured cells were deprived of serum, both ProT α and S100A13 were completely lost from cells at the time point of 3 h. The cellular loss of S100A13 and ProT α was also blocked by amlexanox, a potent inhibitor of S100A13.^{8–11,18} Quantitative immunoblot analysis confirmed that amlexanox abolished the serum-deprivation stress-induced extracellular release of ProT α (Figure 3c).

Protein–protein interaction between ProT α and S100A13. The interaction between ProT α and S100A13 was characterized by use of various deletion mutants of both proteins. In this study, GST-tagged ProT α and *Strep*-tagII-S100A13 were used (Figure 4a). The addition of *Strep*-tagII-S100A13 to GST-ProT α immobilized on the sensor tip of a quartz crystal microbalance (QCM) decreased the quartz oscillation, as quantified by the oscillation unit (OU: ΔF in Hz), which represents the degree of interaction between the two proteins, as reported earlier.¹⁹ The interaction between proteins was enhanced in the presence of Ca²⁺, but not in the presence of Mg²⁺ or Cu²⁺, and this enhancement was Ca²⁺ dependent in the range 0.1–200 μ M (Table 1; Figure 4b). As the Ca²⁺-dependent interaction was further enhanced by the addition of Cu²⁺ (Table 1), which has substantial binding affinity for S100A13, we used the addition of both Ca²⁺ and Cu²⁺ (100 μ M and 100 nM, respectively) to determine the best ionic conditions for the interaction between GST-ProT α and *Strep*-tagII-S100A13. From the kinetic analysis,¹⁹ the saturated OU_{max} for the interaction of *Strep*-tagII-S100A13 with immobilized GST-ProT α (430 fmol) was 201.44 \pm 3.53 OU, which corresponds to

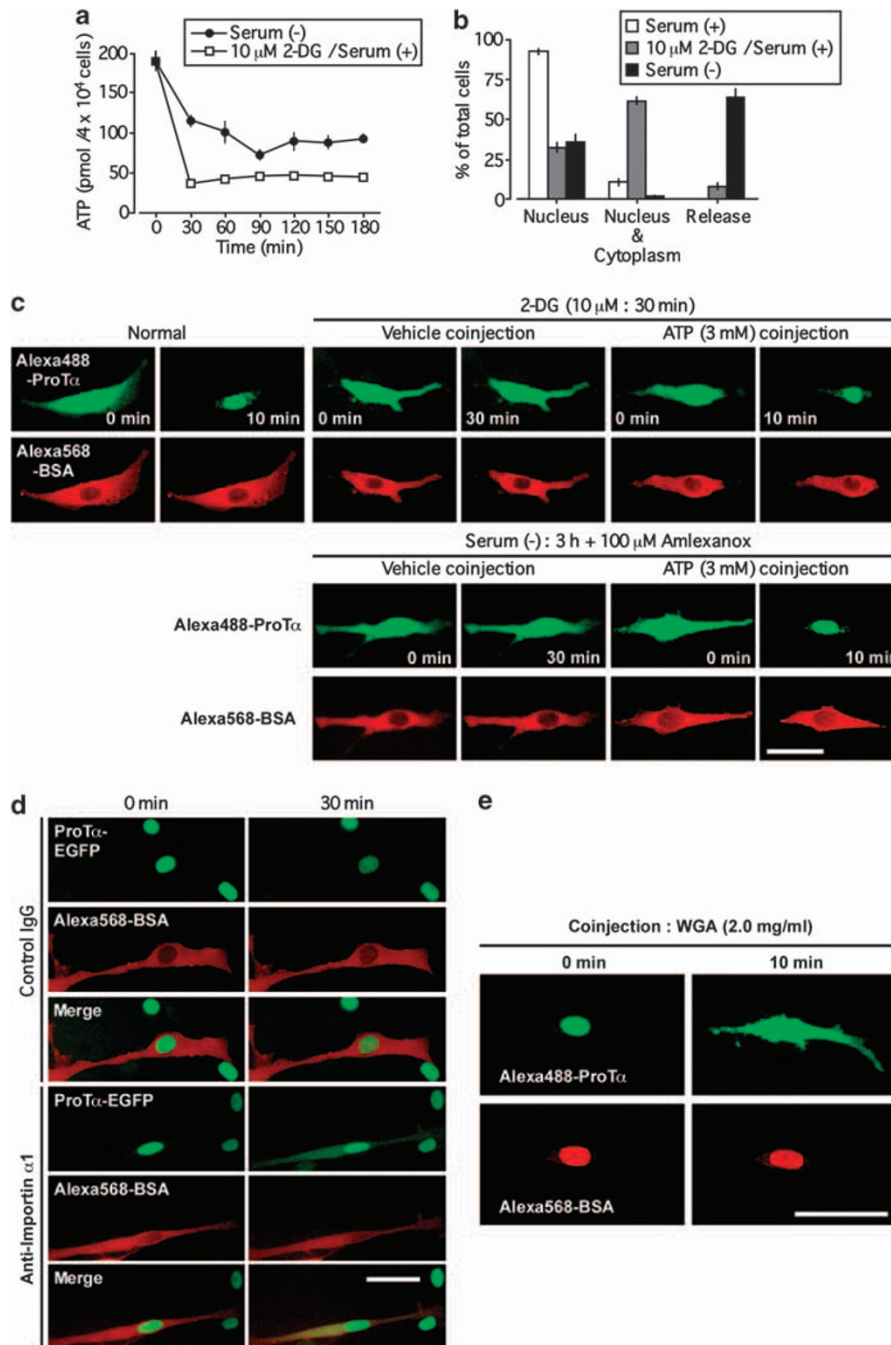


Figure 2 Mechanism underlying the nuclear transport of ProT α . (a) Decrease in intracellular ATP levels induced by serum-deprivation stress. Time courses of intracellular ATP levels were measured in ProT α -EGFP stably expressing C6 glioma cells subjected to serum-deprivation stress or treated with 2-DG (10 μ M, with serum). (b) Altered distribution of ProT α -EGFP by serum (-) or 2-DG treatments (3 h). Distribution of ProT α -EGFP was measured after fixation of C6 glioma cells and visualization of nuclei with Hoechst 33342. Data represent the means \pm S.E.M. of 4–6 independent experiments. (c) ATP-induced recovery of nuclear import of ProT α after 2-DG treatment or serum (-) stress in the presence of amlexanox (100 μ M). Alexa Fluor488-ProT α and Alexa Fluor568-BSA, with or without ATP (3 mM in a needle), were co-injected into cytoplasm. (d) Nuclear import of ProT α mediated by importin α . Importin α , a nuclear transport receptor, binds to classical NLS-containing proteins and links them to the nuclear pore complex. Re-distribution of ProT α -EGFP after cytosolic co-injection of anti-importin α IgG (0.1 μ g/ml in a needle) and Alexa Fluor568-BSA. (e) Passive diffusion of ProT α as a nuclear export mechanism. Injection of wheat germ agglutinin (WGA, 2.0 mg/ml in a needle) into the nucleus induced a re-distribution of ProT α throughout the cell. Scale bars represent 20 μ m

435.63 \pm 7.63 fmol. Therefore, it is evident that ProT α and S100A13 interact at a ratio of 1 : 1.

The C-terminal domains of several types of S100 family proteins are reported to interact with various target proteins.¹⁶

Among these proteins, S100A13 has a unique C-terminal 11-amino-acid sequence (RKEKVLAIRKK), which contains as many as six basic amino acids. In the QCM analysis, *Strep*-tagII-S100A13 lacking this C-terminus (amino-acids

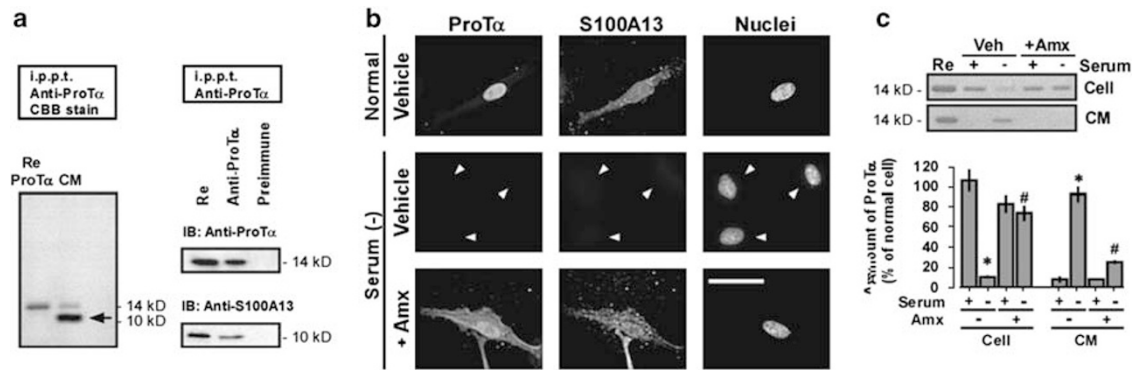


Figure 3 Identification of S100A13 co-released with ProT α on serum-deprivation stress. (a) S100A13 is a major protein interacting with extracellular ProT α . CM from serum-deprived C6 glioma cells (3 h) was subjected to immunoprecipitation with anti-ProT α or pre-immune IgG. Lower band was identified as S100A13 (arrow). Re, recombinant rat ProT α ; IB, immunoblot. (b) Blockade of stress-induced extracellular release of ProT α and S100A13 by amlexanox. Cells were subjected to serum-deprivation stress (3 h) in the presence or absence of amlexanox (Amx; 100 μ M, pretreatment for 30 min). Arrowheads denote the nuclei of cells showing ProT α and S100A13 release. Scale bar represents 20 μ m. (c) Biochemical analysis of amlexanox-induced blockade of serum-deprivation stress-induced extracellular release of ProT α . ProT α in the CM and residual cells was measured by immunoblot. CM was immunoprecipitated with anti-ProT α IgG. Data represent the means \pm S.E.M. of five independent experiments [* and # P < 0.01, versus the corresponding serum (+) and the corresponding Amx (-) treatment, respectively]

88–98) showed no significant interaction with ProT α (Figure 4c). On the other hand, in the experiments using immobilized *Strep*-tagII-S100A13, the C-terminal deletion mutants ProT α (Δ 79–112) and ProT α (Δ 102–112) showed decreased potency for interaction (association rate constant: k_a), whereas the N-terminal deletion mutants ProT α (Δ 1–68) and ProT α (Δ 1–86) did not (Figure 4d). As the C-terminal peptide ProT α (amino-acids 102–112; TKKQKKTDEDD), but not its reverse peptide (DDEDTKKQKKT), inhibited the interaction between GST-ProT α and *Strep*-tagII-S100A13 (Figure 4e), the C-terminal sequence appears to have a crucial function in this interaction. On the contrary, the N-terminal region is presumed to have an unidentified regulatory function in this interaction.

Interaction between ProT α and S100A13 is required for the extracellular release of ProT α . To confirm that the stress-induced extracellular release of ProT α depends on the ProT α –S100A13 interaction, we established C6 glioma cells stably expressing *Strep*-tagII-S100A13 Δ 88–98, which lacks affinity for ProT α . In the immunocytochemical study, serum-deprivation stress caused an extracellular release of both ProT α and *Strep*-tagII-S100A13 full-length mutant from C6 glioma cells (Figure 5a, left panels, and 5b). However, with the *Strep*-tagII-S100A13 Δ 88–98 mutant, serum-deprivation stress caused the release of the mutant protein, but not ProT α (Figure 5a, right panels, and 5b). This finding suggests that the C-terminal basic residue-rich domain of S100A13 is required for the interaction with ProT α in living cells, and that S100A13 has a function as a cargo molecule involved in the extracellular export of ProT α . To identify the intracellular locales of interaction between ProT α and S100A13, we performed *Strep*-tagII pull-down assay using nuclear and cytosolic fractions from C6 glioma cells stably expressing *Strep*-tagII-S100A13 (Figure 5c). In the absence of stress, there was no interaction between *Strep*-tagII-S100A13 and ProT α in either nuclear or cytosolic fraction. Under the serum-deprivation stress, however, a significant interaction was

observed in the cytosol fraction, but not in the nuclear one. The level of co-precipitated ProT α in the cytosol was decreased in a time-dependent manner in the range between 1 and 3 h, possibly because of the loss of cytosolic ProT α by extracellular release of both proteins. To evaluate the ProT α –S100A13 interaction in living cells, we performed fluorescence resonance energy transfer (FRET) analysis. However, the representative FRET analysis using a pair of CFP and YFP was not successful, because the YFP-fused ProT α showed an abnormal distribution. Instead, we attempted to assess the interaction between ProT α -EGFP and DsRed2-S100A13 in the presence of amlexanox, which has no direct effect on their interaction (Table 1). In addition, we performed using phenol red-free DMEM, which does not decrease the survival activity of C6 glioma cells under serum-deprivation condition (Supplementary Figure S1). In the cell population, FRET analysis in the presence of amlexanox, the serum-deprivation stress-induced interaction between ProT α and S100A13 (Figure 5d), and ProT α and S100A13 were redistributed throughout the cell (Figure 5g). To calculate the FRET efficiency, we performed acceptor photo-bleaching. When the acceptor (DsRed2-S100A13) was earlier bleached, serum-deprivation stress did not cause elevation of FRET ratio; however, ProT α and S100A13 were also redistributed throughout the cell (Figure 5d and g). Next, we performed the single cell FRET analysis in the absence of amlexanox. As shown in Supplementary Figure S2a, the FRET ratio in the cytosol was rapidly increased at 80 min after serum deprivation, whereas then gradually decreased, possibly because of the extracellular release of ProT α –S100A13 complex. In accord with this observation, the fluorescence intensity derived from donor ProT α -EGFP decreased at 80 min, whereas the one derived from acceptor DsRed2-S100A13 transiently increased (Supplementary Figure S2b). These results strongly suggest that the interaction between ProT α -EGFP and DsRed2-S100A13 occurs in the cytosol. As shown in Figure 5e, the serum-deprivation stress-induced interaction

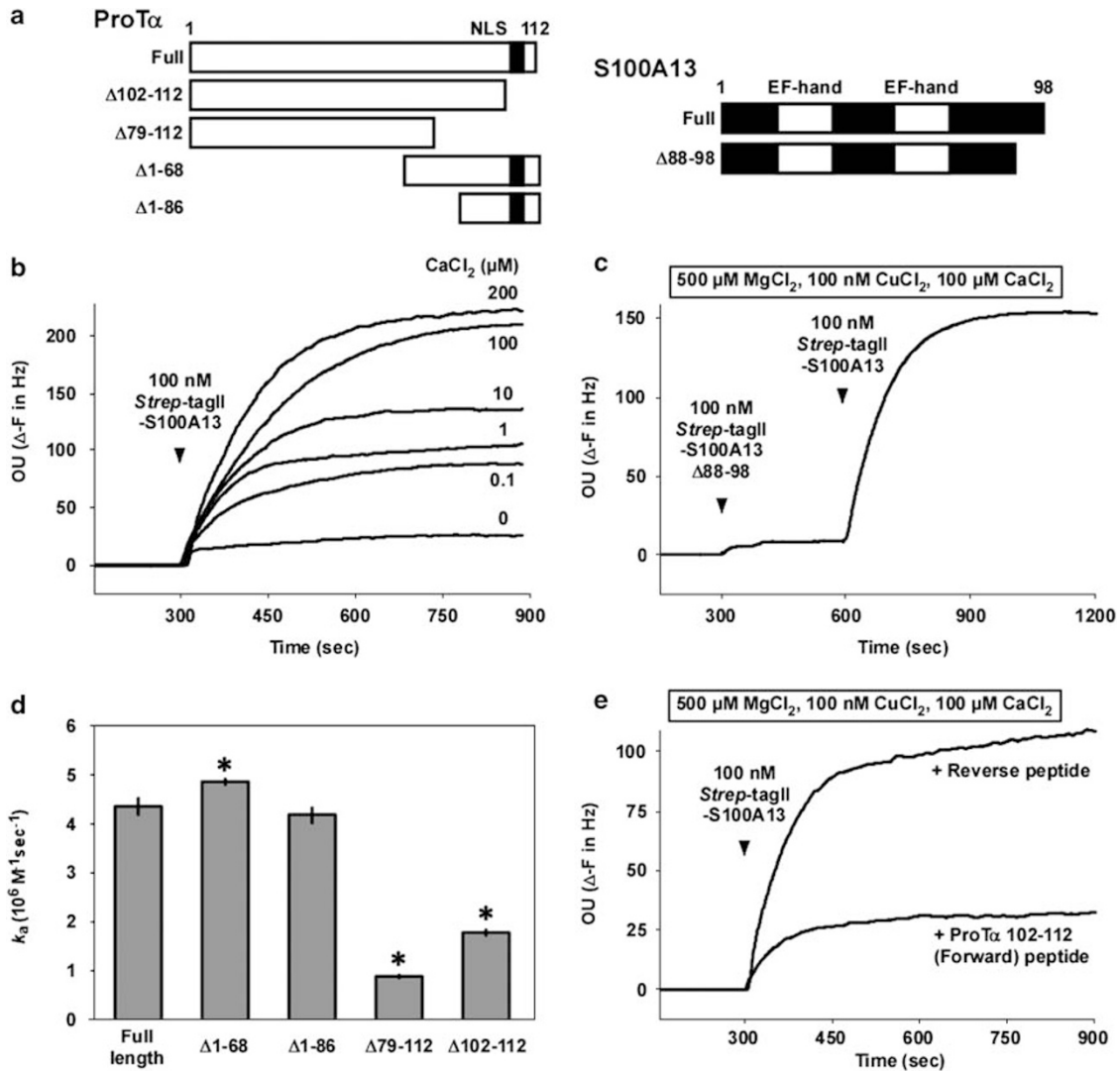


Figure 4 Biochemical interaction between GST-ProT α and *Strep*-tagII-S100A13, evaluated by QCM. (a) ProT α and S100A13 mutant constructs. (b) The interaction between GST-ProT α and *Strep*-tagII-S100A13 occurs in a Ca²⁺ concentration-dependent manner. The time course of the interaction in the presence of various concentrations of Ca²⁺ (0–200 μ M) was measured. (c) Loss of interaction between S100A13 lacking the C-terminal region (Δ 88–98) and ProT α . (d) Loss of interaction between GST-ProT α deletion mutants lacking C-terminal regions and *Strep*-tagII-S100A13. Data represent the means \pm S.E.M. of five independent experiments (* P < 0.05, versus full length). (e) Interference by ProT α C-terminal forward peptide (amino-acids 102–112). Arrowheads represent the application points of *Strep*-tagII-S100A13 mutants

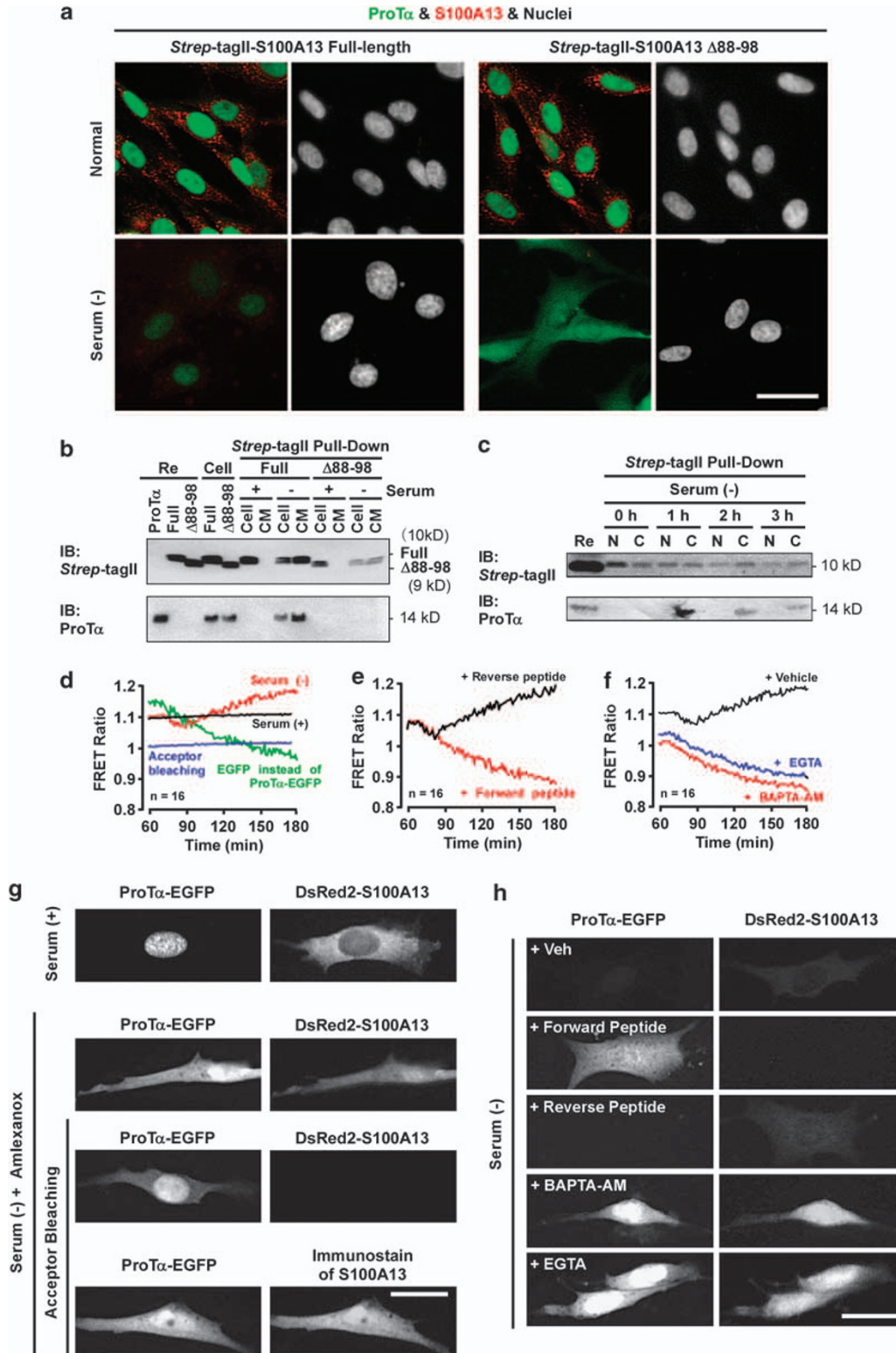
Table 1 The association rate constant (k_a) and dissociation constant (K_D) value of *Strep*-tagII-S100A13 for GST-ProT α in the QCM assay

	Mg ²⁺ (μ M)	Ca ²⁺ (μ M)	Cu ²⁺ (μ M)	Amlexanox (100 μ M)	k_a (10 ⁴ /M/s)	K_D (10 ⁻⁸ M)
A	0	0	0	–	1.98 \pm 0.28	21.19 \pm 3.43
B	100	0	0	–	1.83 \pm 0.31	27.66 \pm 6.52
C	0	100	0	–	10.03 \pm 0.14**	6.98 \pm 0.09**
D	0	0	100	–	3.40 \pm 0.52	13.62 \pm 3.03
E	500	100	0	–	7.01 \pm 0.21	5.72 \pm 0.17
F	500	100	0.1	–	9.46 \pm 0.23*	3.20 \pm 0.68*
G	500	100	0	+	6.84 \pm 0.06	5.89 \pm 0.18
H	500	100	0.1	+	9.88 \pm 0.43*	4.38 \pm 0.20*

The interaction between ProT α and S100A13 was in a Ca²⁺-dependent manner. The interaction was analyzed by both GST-ProT α and *Strep*-tagII-S100A13. GST-ProT α was immobilized on the anti-GST antibody-coated sensor chip, hence orientation of ProT α (host sample) was fixed. The k_a and K_D values were obtained by the analysis using cumulative application of *Strep*-tagII-S100A13 (guest sample). Cu²⁺ potentiated the Ca²⁺-dependent interaction between GST-ProT α and *Strep*-tagII-S100A13. Amlexanox did not affect this interaction. Each experiment was analyzed in interaction buffer. The data shown are mean \pm S.E.M. of 3–5 independent experiments. * P < 0.05 and ** P < 0.01 versus corresponding control (A and E)

between ProT α and S100A13 was abolished by the C-terminal (102–112) peptide of ProT α , but not by the reverse peptide. The treatment with C-terminal peptide inhibited the serum-

deprivation-induced extracellular release of ProT α , but not S100A13, whereas the reverse peptide did not inhibit the extracellular release of either protein (Figure 5h, upper 6 panels).



Ca²⁺ influx is involved in the extracellular release of ProT α based on the interaction with S100A13. In the FRET analysis (Figure 5f), the serum-deprivation stress-induced interaction between ProT α and S100A13 was abolished when the cells were treated with EGTA or BAPTA-AM, extracellular and intracellular Ca²⁺-chelating agents, respectively. The serum-deprivation-induced loss of these proteins was also abolished by EGTA or BAPTA-AM (Figure 5h, lower 4 panels).

Caspase-catalyzed cleavage of ProT α inhibits the stress-induced extracellular release. When C6 glioma cell culture was carried out in various concentrations of serum, significant depletion of ProT α was observed in the absence of serum, but not in the presence of 2 or 10% serum (Figure 6a, upper 6 panels, and 6b). When staurosporine, tunicamycin, and etoposide, which are known to induce apoptosis, were added to 2% serum medium, ProT α was redistributed throughout the cell (Figure 6a, middle 6 panels). However, these apoptogenic compounds did not cause any significant extracellular release of ProT α , but led to the production of large amounts of a smaller ProT α fragment (Figure 6b). These re-distribution and fragmentation of ProT α were in a caspase-3 inhibitor zDEVD-fmk-reversible manner (Figure 6a, lower 6 panels and 6b). On the other hand, these compounds did not affect intracellular ATP levels (Supplementary Figure S3).

When rat ProT α was treated with active caspase-3, a 13 kDa protein band was time dependently generated in a zDEVD-fmk-reversible manner (Figure 6c). This finding is consistent with reports that human ProT α has three overlapping caspase-3 cleavage sites, 94DDED97, 95DEDD98, and 97DDVD101,^{20,21} immediately upstream of the NLS moiety in its C-terminus, and that this fragment lacks an NLS moiety KKQK, which is present in rat ProT α at amino-acid positions 103–106. To identify the cleavage sites of rat ProT α by active caspase-3, we performed MALDI-TOF analysis. As shown in Figure 6e, MALDI-TOF analysis revealed that the molecular mass of purified ProT α in naive C6 glioma cells was 12259.99, which corresponds to N-terminal serine acetylated full-length size (Ac2-112), whereas ProT α -like molecule in apoptogenic staurosporine-treated cells was 10480.39 or 10596.43, which corresponds to C-terminal truncated ProT α

Ac2-97 or Ac2-98, respectively. Tunicamycin or etoposide treatments also showed similar results (data not shown). Next, we tried to characterize the cleavage region of recombinant rat ProT α (rrProT α) by caspase-3 by use of peptide mass fingerprinting analysis. In this experiment, rrProT α was incubated with or without active rat caspase-3, followed by a separation with SDS-PAGE, in-gel digestion of protein bands with trypsin and MALDI-TOF analysis (Figure 6f). In the absence of incubation of active rat caspase-3 (blue peaks), two peaks with molecular mass of 1131.15 and 1479.66 were identified as a.a.22–31 and a.a.91–103 peptides, respectively. However, in its presence (black peaks), there were new peaks with 792.47 and 907.41, corresponding to a.a.91–97 and a.a.91–98 peptides, respectively, but the peak with 1479.66 disappeared. Furthermore, the digestion of synthetic rat ProT α C-terminal 93–112 polypeptide by caspase-3 produced two peaks with molecular mass of 1678.88 and 1794.01, which correspond to a.a.99–112 and a.a.98–112 peptides, respectively (Figure 6g). All these results indicate that rat ProT α has the two overlapping cleavage sites by caspase-3 (Figure 6d). Accordingly, ProT α likely loses its NLS moiety under apoptotic conditions. This view is supported by the finding that immunoreactive ProT α is no longer localized in the nucleus after treatment of cells with apoptogenic compounds (Figure 6a). On the basis of the finding that the ProT α fragment was not released from cells, this C-terminal region appears to be essential for the extracellular release of ProT α .

Discussion

The nuclear protein ProT α currently attracts the interest of investigators in terms of life and death decisions in various cell types. In the nucleus, this protein epigenetically stimulates cell proliferation by binding to histones,²² p300 histone acetyltransferase,²³ and CREB-binding protein.²⁴ ProT α also enhances estrogen receptor transcriptional activity by binding to its repressor,²⁵ and binds to Keap1 to release Nrf2, which in turn upregulates various kinds of anti-oxidant enzymes important for survival.²⁶ Under the apoptotic conditions, it inhibits apoptosome formation.⁴ Most recently, we discovered this protein as an anti-necrosis factor in the CM of cultured cortical neurons under serum-free starving conditions causing

Figure 5 S100A13 is a cargo molecule mediating extracellular ProT α release. (a) S100A13 Δ 88–98 mutant as a dominant-negative regulator of ProT α release. Distributions of ProT α and *Strep*-tagII-S100A13 mutants in cultured C6 glioma cells with or without serum. (b) Loss of interaction of the *Strep*-tagII-S100A13 Δ 88–98 mutant with ProT α in living cells. Cells and CM from C6 glioma cells stably expressing *Strep*-tagII-S100A13 mutants with or without serum (3 h) were harvested and a *Strep*-tagII pull-down assay was performed. Re: recombinant rat proteins. (c) The interaction of the *Strep*-tagII-S100A13 with ProT α occurs in cytosol, but not nucleus. Nucleus (N) and cytosol (C) from C6 glioma cells stably expressing *Strep*-tagII-S100A13 mutants with or without serum (3 h) were prepared and a *Strep*-tagII pull-down assay was performed. (d–f) Imaging of the ProT α -S100A13 interaction in living cells. Time-course of FRET images after serum-deprivation stress in phenol red-free DMEM. DsRed2-S100A13 was transiently expressed in C6 glioma cells stably expressing ProT α -EGFP. The FRET ratio represents the emission ratio of 590/520 nm. (d) Serum-deprivation stress-induced increase in the FRET emission ratio. Cell population images of FRET were measured in the presence of amlexanox (100 μ M). Serum-deprivation stress caused an increase in the emission ratio from approximately 90 min. When the acceptor (DsRed2-S100A13) was earlier bleached, serum-deprivation stress did not increase the emission ratio. In cells expressing EGFP instead of ProT α -EGFP, FRET did not occur after serum deprivation. (e) Inhibition of FRET by the ProT α C-terminal peptide. Cellular delivery of a C-terminal peptide (amino-acids 102–112; forward peptide) of ProT α abolished increase of FRET emission ratio and decreased basal level, whereas no change was observed with the reverse peptide. (f) Inhibition of FRET by Ca²⁺ chelating. Cytosolic and extracellular Ca²⁺-chelating agents, BAPTA-AM, and EGTA, respectively, inhibited FRET after serum deprivation. A decrease in the basal level of the emission ratio was observed approximately 70 min after the stress, suggesting that nuclear ProT α -EGFP is redistributed into the cytosol, but does not interact with S100A13 in the absence of Ca²⁺. BAPTA-AM and EGTA were used at 1 μ M and 1 mM, respectively. (g) Subcellular distribution of ProT α -EGFP and DsRed2-S100A13. The images were collected 180 min after serum deprivation after FRET analysis. (h) Inhibition of extracellular release of ProT α -EGFP and DsRed2-S100A13. The images were collected 180 min after serum-deprivation stress. Scale bars represent 20 μ m

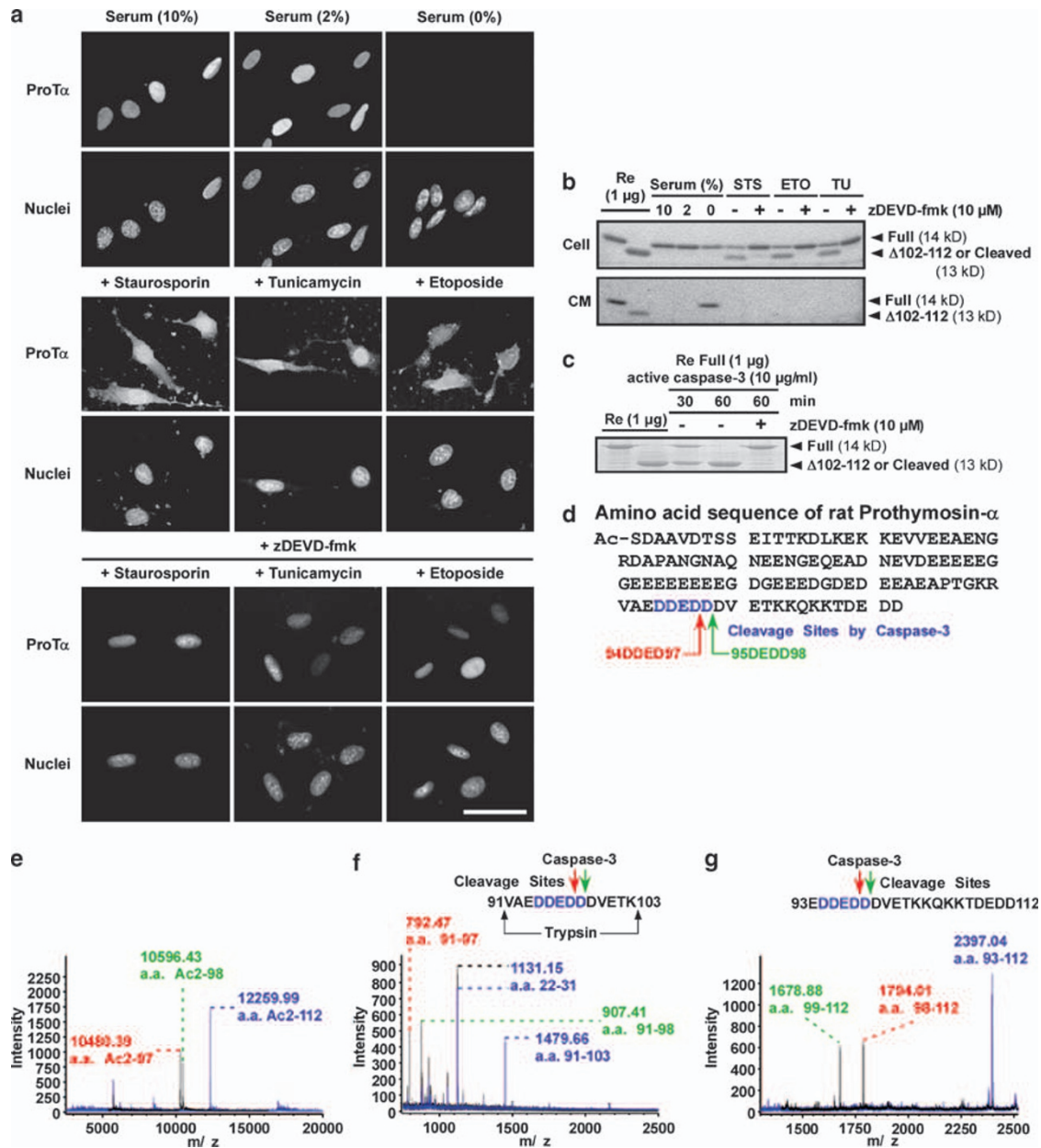


Figure 6 Apoptotic stress induces re-distribution of ProT α . **(a)** Altered distribution of ProT α in C6 glioma cells. Cells were subjected to serum-reduced (2%) or serum-deprivation stress for 3 h. Cells were treated with staurosporine, tunicamycin, or etoposide for 3 h in the presence or absence of zDEVD-fmk (10 μ M). All apoptogenic compounds were used at 1 μ M in 2% serum-containing medium. Scale bars represent 20 μ m. **(b)** Cleavage, but not release of ProT α by apoptogenic compounds treatment. STS, staurosporine; TU, tunicamycin; ETO, etoposide. **(c)** Rat ProT α as a caspase-3 substrate. Recombinant (Re) rat ProT α (1 μ g) was incubated with 10 μ g/ml recombinant active caspase-3 in the presence or absence of 10 μ M zDEVD-fmk for 1 h at 37°C. Recombinant rat ProT α Δ 102–112 mutant was used as a marker of ProT α fragment lacking the C-terminal region. **(d)** Cleavage sites of rat ProT α by active caspase-3. **(e–g)** Identification of cleavage sites of rat ProT α by active caspase-3 by use of MALDI-TOF analysis. **(e)** Generation of two truncated types of ProT α by apoptogenic compound treatment. Peaks of intracellular native ProT α and cleaved ProT α by staurosporine treatment were shown as blue and black, respectively. The molecular mass of 12259.99 represents N-terminal serine acetylated full-length size (Ac2-112). The molecular mass of 10480.39 or 10596.43, which corresponds to C-terminal truncated ProT α Ac2-97 or Ac2-98, respectively. **(f)** Characterization of cleavage of ProT α by caspase-3 by peptide mass fingerprinting. Recombinant rat ProT α was incubated with or without active rat caspase-3, followed by a separation with SDS-PAGE, in-gel digestion of protein bands with trypsin and MALDI-TOF analysis. In the absence of incubation of active rat caspase-3 (blue peaks), two peaks with molecular mass of 1131.15 and 1479.66 were identified as a.a.22–31 and a.a.91–103 peptides, respectively. However, in its presence (black peaks), there were new peaks with 792.47 and 907.41, corresponding to a.a.91–97 and a.a.91–98 peptides, respectively, but the peak with 1479.66 disappeared. **(g)** Cleavage of rat ProT α C-terminal regions by active caspase-3. Blue peak with molecular mass of 2397.04 represents synthetic rat ProT α C-terminal 93–112 polypeptide. The digestion of C-terminal polypeptide by caspase-3 produced two peaks with molecular mass of 1678.88 and 1794.01, which correspond to a.a.99–112 and a.a.98–112 peptides, respectively

necrosis.⁵ Extracellular ProT α completely inhibits neuronal necrosis, but causes apoptosis in a different manner in cultured neurons.^{27–29} However, after stroke, endogenous

neurotrophins, such as brain-derived neurotrophic factor (BDNF) or erythropoietin, have been found to inhibit the apoptosis induced by exogenously administered ProT α .⁶ In

the retinal ischemia model, the ischemic stress depletes ProT α from the retinal cells, and the intravitreal pretreatments with anti-ProT α IgG or antisense oligodeoxynucleotide against ProT α deteriorated the ischemic damage.⁷ Therefore, it is evident that ProT α is extracellularly released from nuclei on ischemic stress, and that it exerts endogenous neuroprotective functions.

Polypeptide secretion has largely been defined as a process of exocytosis through the fusion of vesicles containing bioactive substances to the plasma membrane. In the representative vesicular secretion pathway, polypeptides that possess a signal peptide sequence in their N-terminal region are sorted to the ER-Golgi system to be processed by exocytosis.^{30,31} However, several polypeptides possess extracellular functions despite lacking a signal sequence. The extracellular release of such polypeptides has to proceed through ER-Golgi-independent or non-vesicular (so-called non-classical) routes. It should be noted that these polypeptides showing non-classical extracellular release in general have significant functions in the life and death decisions of cells, as seen in the cases with angiogenic growth factors, inflammatory cytokines, extracellular matrix growth factors, viral proteins, and parasite surface proteins.^{32,33} Unlike vesicular release, this type of release is caused by non-physiological stressful stimuli, which may cause rapid cell death. A series of pioneering studies by Maciag and his coworkers led to the hypothesis that S100A13 has key functions in the so-called non-classical extracellular release.⁸ S100A13 has two EF-hand Ca²⁺-binding motifs and belongs to a member of the S100 family.^{15–17} It has been reported that S100A13 is involved in the non-classical extracellular release of target molecules containing fibroblast growth factor-1 (FGF-1) and interleukin-1 α .^{9–11,19,34,35} In this study, we successfully showed that ProT α is another example of stress-induced non-vesicular extracellular release, using S100A13, a cargo molecule. Furthermore, we revealed that the C-terminal regions of ProT α and S100A13 are essential for their interaction, which precedes extracellular release of both proteins, and that caspase-3 cleaves off C-terminal regions of ProT α . Thus, the non-vesicular extracellular release of ProT α has a unique feature that it does not occur under the condition of apoptosis.

The unique point in this study is observed in the fact that ProT α is strictly localized in the nucleus in neurons, astrocytes, and C6 glioma cells. The mechanism underlying ischemic stress-induced extracellular release of ProT α comprises a two-tier export system: from the nucleus to the cytosol, and from the cytosol to outside the cell. As mentioned above, the nuclear export of ProT α is attributed to ischemia-induced ATP loss, which impairs the importin-NLS mechanism. As this nuclear export was not affected by leptomycin B, the serum-deprivation stress-induced drastic decrease in nuclear levels of ProT α is likely to be due to passive diffusion. Interestingly, once ProT α is exported from the nucleus, it is disappeared without remaining in the cytosol. In other words, nuclear export is the rate-limiting step for non-vesicular and extracellular release of ProT α .

The stress-induced extracellular release of ProT α was impaired by the addition of cytosolic or extracellular Ca²⁺-chelating agents. The interaction between ProT α and

S100A13 was Ca²⁺ concentration dependent in the range 0.1–200 μ M, which corresponds to the cellular levels between resting and stimulated conditions. The Ca²⁺ dependency seems to be attributed to the facts that both S100A13 and ProT α are Ca²⁺-binding proteins.^{15–17,36} On the basis of the observation that serum-deprivation stress causes the activation of voltage-dependent N-type Ca²⁺ channel, which is involved in the non-classical release of FGF-1 and S100A13,^{34,35} ischemic stress-induced Ca²⁺ influx may underlie the non-vesicular ProT α release as the second step after ATP loss-dependent nuclear release.

Neurons die by necrosis in the low density of culture under the serum-starved condition, but their survival activity increases as the cell density goes. We identified ProT α as the important molecule, which is released in the CM of serum-starved culture of neurons, and suppresses the necrosis through a recovery of glucose transport and ATP supply.^{5,37} After longer culture with ProT α , however, we found that neurons die by apoptosis through activation of caspase-3.⁵ As caspase-3 is known to cleave poly-[ADP-ribose] polymerase, which consumes abundant ATP molecule for the restoration from stress-induced damage of DNA,³⁸ this machinery seems to have some functions in suppression of rapid necrosis by stress.²⁹ As the concomitant addition of anti-apoptotic neurotrophins with ProT α completely inhibits the cell death, the physiological meaning of ProT α action would be speculated as a conversion of uncontrollable cell death necrosis to controllable apoptosis. Indeed, this speculation was confirmed by *in vivo* study, in which exogenous ProT α inhibited both necrosis and apoptosis of retinal cells after ischemia, but the further treatment with anti-BDNF antibody disclosed the apoptosis induction by ProT α .⁷

It should be noted that ProT α in the cytosol inhibits apoptosis through an inhibition of apoptosome formation in non-neuronal HeLa cells.⁴ Furthermore, there is a report that ProT α is released from the nuclei when the NLS is cleaved off by caspase-3.^{20,21} This study clearly showed that the C-terminal region of ProT α including NLS is cleaved in culture by the apoptosis-induced compound, and in cell-free digestion of recombinant ProT α by active caspase-3 (Figure 6d–g). As ProT α devoid of C-terminal region (a.a.98 or 99–112) is conceived to lose the activity of interaction with S100A13 (Figure 4d), it will remain in the cytosol without extracellular release. All these findings enable us to speculate that ProT α extracellularly released on the necrosis condition inhibits neuronal necrosis in an autocrine or paracrine manner, whereas cytosolic ProT α redistributed from the nuclei on the apoptotic condition may have an anti-apoptotic self-defensive function.

It is well known that several endogenous molecules are released in response to injury, infection, or other inflammatory stimuli, and initiate inflammatory responses. These molecules are so-called damage-associated molecular patterns (DAMPs) and/or alarmins.^{39,40} Although DAMPs have intranuclear and/or intracellular functions under normal conditions, they have extracellular effects under pathological conditions. High-mobility group box1 (HMGB1), a representative DAMP molecule, has similar characteristics to ProT α . HMGB1, a nuclear protein, is released by necrotic stress, but not by apoptosis, as seen for ProT α . However, it causes

cell damaging or inflammatory actions. Although this release is reported to occur through passive diffusion through necrosis-induced membrane disruption, detailed characterization of the mechanism is required. It is interesting to propose that ProT α is a novel type of DAMP bearing cell-defensive functions in brain.

In conclusion, we showed that the nuclear protein ProT α is extracellularly released from neurons, astrocytes, and C6 glioma cells on ischemic stress in a non-vesicular manner. The initial step of this release is nuclear release of ProT α owing to the stress-induced ATP loss. Non-vesicular extracellular release of ProT α is dependent on a Ca²⁺-sensitive interaction with S100A13. We also showed that ProT α loses the ability to undergo extracellular release under apoptotic conditions, owing to loss of its interaction with S100A13, a cargo molecule.

Materials and Methods

Materials and antibodies. Brefeldin A was purchased from Nacalai Tesque (Kyoto, Japan). The 2-DG, staurosporine, tunicamycin, etoposide, and leptomycin B were purchased from SIGMA (St. Louis, MO, USA). Wheat germ agglutinin was purchased from Biomeda Corp. (Burlingame, CA, USA). Amlexanox was kindly provided by Takeda Pharmaceutical Company Ltd. (Osaka, Japan). Rat ProT α C-terminal synthetic peptides (amino-acids 102–112: forward sequence, TKKQKKTDEDD; reverse sequence, DDEDTKKQKKT; amino-acids 93–112: forward sequence, EDDEDDVETKKQKKTDEDD) were purchased from Bio Synthesis Inc. (Lewisville, TX, USA). Mouse anti-ProT α antibody was kindly provided by Dr. AB Vartapetian (Moscow State University, Moscow, Russia) or purchased from Alexis Biochemicals (Lausen, Switzerland). These two antibodies are derived from the same source. Goat anti-importin α 1 and normal goat antibody were purchased from Santa Cruz Biotechnology Inc. (Santa Cruz, CA, USA) and ICN/Cappel Inc. (Durham, NC, USA), respectively. Rabbit anti-S100A13 antibody was kindly provided by Dr. T Maciag (Center for Molecular Medicine, Maine Medical Center Research Institute, Scarborough, ME, USA).

Expression constructs and purification procedures for proteins. The rat ProT α gene was amplified from cDNA derived from rat embryonic brain. The PCR primers used were ProT α -F, 5'-AACATATGTCA GACGCGCAGTGGGA-3' (containing a NdeI site), and ProT α -R, 5'-AAGGATC CAGTGGAGGGTGAATAGGTCAC-3' (containing a BamHI site). Recombinant ProT α protein was constructed by cloning the amplified ProT α gene in-frame into the NdeI-BamHI sites of pET-20b (Novagen, San Diego, CA, USA). Native and recombinant ProT α were purified using a phenol extraction procedure⁴¹ and visualized with Coomassie Brilliant Blue (Gelcode blue stain reagent; PIERCE Biotechnology, Rockford, IL, USA). Recombinant GST-ProT α deletion mutants were constructed by cloning the amplified genes blunted at their 5'-ends and cloned in-frame into the BamHI (blunted)-EcoRI sites of pGEX-5X-1 (GE Healthcare Bio-Science Corp., Piscataway, NJ, USA). The PCR primers used were as follows: Full-F, 5'-AGGGATCCAATGTGCAGCGCGCAGAG-3'; Δ 1–68-F, 5'-AGGGATCCAATGGAAGGTGATGGTGAGGAAG-3'; Δ 1–86-F, 5'-AGGGAT CCAATGACGGCAAGCGGGTAGCTG-3'; Full-R, 5'-TTGAATTCCTAGTCATCC TCATCAGTCTTC-3'; Δ 79–112-R, 5'-TTGAATTCCTAATCTCCATCTTCTTCCTC-3'; and Δ 102–112-R, 5'-TTGAATTCCTACTCAACATCATCCTCATC-3'. All F-primers contain a BamHI site, whereas all R-primers contain a stop codon and an EcoRI site. The recombinant proteins were purified using Glutathione-Sepharose (GE Healthcare Bio-Science Corp.). An EGFP-ProT α fusion protein, for mammalian expression, was constructed by cloning the amplified genes in-frame into the SacI-SalI sites of pEGFP-N3 (BD Bioscience Clontech, Palo Alto, CA, USA). The PCR primers used were ProT α -F2, 5'-AAGAGCTCATGTGCAGCGCGCAGTGGGA-3' (containing a SacI site), and ProT α -R2, 5'-AAGTCGAGTCATCCTCATCAG TCTTCT-3' (containing a SalI site). Plasmid construction and purification procedure of recombinant *Strep-tagII*-S100A13 protein (full length and Δ 88–98) were performed as described earlier.³⁴ DsRed2-S100A13 fusion protein, for mammalian expression, was constructed by cloning. The rat S100A13 gene was amplified from cDNA derived from rat embryonic brain. The PCR primers used were S100A13-F, 5'-AAGAATTCATGGCAGCAGAGCCCGAC-3', and S100A13-R,

5'-AAAAGCTTTTACTTCTTGCAGATCGCCAGG-3'. The amplified S100A13 gene was cloned into pGEM-T Easy (Promega, Tokyo, Japan), and sub-cloned in-frame into the NotI-SpeI sites of pBluescript SK (Stratagene, La Jolla, CA, USA). Finally, the S100A13 gene was sub-cloned in-frame into the SacI-BamHI sites of pDsRed2-C1 (BD Bioscience Clontech). After cloning, each construct was verified by sequencing. The *Escherichia coli* strains DH10B and BL21 (DE3) were transformed with each of these constructs for sub-cloning and protein expression, respectively. For the analysis of protein–protein interactions and their modulation by ions, we adopted the following molecular weight values (average mass) for full-length GST-ProT α and *Strep-tagII*-S100A13, Ca, and Cu: 39 016.19, 13 840.08, 40.078, and 63.546, respectively.

Cell culture, gene transfection, and peptide delivery. Primary cultures of neurons and astrocytes from 17-day-old embryonic rat brain, and cultures of C6 glioma cells, were prepared as described earlier.^{34,42} Gene constructs were transfected with the NeuroPORTER reagent (Gene Therapy Systems, Inc., San Diego, CA, USA). C6 glioma cells stably expressing recombinant protein were selected and maintained in 1 mg/ml G418. Recombinant protein expression was confirmed in isolated clones by microscopy and by immunoblotting. Synthetic peptides were delivered into living cells using the BioPORTER protein delivery reagent (Gene Therapy Systems, Inc.).

Immunocytochemistry. Cells were fixed in 4% paraformaldehyde in PBS for 30 min and then permeabilized with methanol for 10 min at room temperature. The fixed cells were washed with PBS, incubated in blocking buffer (1% BSA and 0.1% Triton X-100 in PBS) for 3 h at 4°C, and then incubated in primary antibody (1 : 300 dilution in blocking buffer) overnight at 4°C. Next, the cells were incubated in a secondary antibody conjugated to FITC or Cy3 (Chemicon International Inc., Temecula, CA, USA), and then with rhodamine-conjugated streptavidin (Chemicon International Inc.), each diluted 1 : 500 in blocking buffer. The nuclei were visualized with Hoechst 33342 or propidium iodide (Molecular Probes, Eugene, OR, USA). Images were collected using a BZ-8000 microscope (KEYENCE, Osaka, Japan) with a \times 20 Plan APO lens (Nikon, Tokyo, Japan) or using an LSM 510 META confocal laser microscope with a \times 40 Plan-Neofluar lens or a \times 63 Plan-Apochromat lens (Carl Zeiss, Oberkochen, Germany).

Gravimetric measurements with a biosensor QCM. Protein–protein interactions were detected using an AffinixQ system (Initium Inc., Tokyo, Japan), a QCM sensor device. Detailed procedures have been described earlier.¹⁹ AT-cut quartz crystals coated with a thin gold surface layer with a fundamental frequency of 27 MHz were used. Immediately before use, the gold surface of the quartz resonator was cleaned with piranha solution (H₂SO₄: 30% H₂O₂ = 3 : 1) for 5 min, and thoroughly washed with double-distilled water. An anti-GST antibody (GE Healthcare Bio-Sciences Corp.) or a streptavidin-conjugated antibody solution (ICN/Cappel Inc.) was applied to the resonator for 30 min to obtain a layer for immobilization of GST-ProT α or *Strep-tagII*-S100A13, respectively. Next, the resonator was rinsed with interaction buffer (50 mM Tris–HCl pH 7.6, 15 mM NaCl, 140 mM KCl), immersed in interaction buffer (8 ml), and then subjected to immobilization of GST-ProT α or *Strep-tagII*-S100A13 for 30 min before being placed in fresh interaction buffer. The protein–protein interactions were determined from the frequency changes (OU: ΔF in Hz) owing to changes in the mass on the electrode at the sub-nanogram level, on application of a small volume (1–10 μ l) of protein solution. On the basis of the Sauerbrey formula, an increase of 1 Hz OU is calculated as an interaction of 30.38 pg of a molecule with the biosensor. In all immobilizations of GST-ProT α on the resonator, it was confirmed that approximately 430 fmol of GST-ProT α was immobilized as an absolute amount (an increase of OU: 550 Hz). All experiments were carried out at 25 ± 1 °C. All sensorgram data show the OU value after the association phase. For kinetic analysis, frequency changes induced by cumulatively applied protein were curve fitted to the formula $\Delta F = A(e^{-(1/\tau)T} - 1)$, and the $1/\tau$ value was plotted for each concentration of added protein. $1/\tau$ and K_D represent $k_a[X] + k_d$ and k_d/k_a , respectively, where X is the concentration of the added protein. K_D , k_a , and k_d denote dissociation constant, association rate constant, and dissociation rate constant, respectively.

Co-immunoprecipitation analysis and *Strep-tagII* pull-down assay. For the determination of protein release, cell lysis buffer (150 mM NaCl, 1 μ M CaCl₂, 50 mM Tris–HCl pH 7.8, 1% Triton X-100, and protease inhibitor cocktail) was added to cells ($0.5\text{--}2 \times 10^6$ cells) to a final volume of 1 ml and the samples were sonicated. Cells and CM (1 ml) samples were used after the removal

of insoluble debris by centrifugation at $10\,000 \times g$. For immunoprecipitation analysis, anti-ProT α or pre-immune antibodies and protein G-Sepharose beads (GE Healthcare Bio-Science Corp.) were added to CM and incubated on a rotor for 2 h at 4°C. For preparation of nuclear and cytosolic fractions, cells were harvested by cell lysis buffer and then homogenized by dounce homogenizer. Nuclear fraction was collected by centrifugation at $1000 \times g$ and supernatant fluid was used as cytosolic fraction. For the Strep-tagII pull-down assay, StrepTactin-Sepharose beads were added to cells or CM samples and incubated on a rotor for a further 1 h at 4°C. The beads were washed three times with lysis buffer and quenched with 50 μ l of SDS sample buffer.

Immunoblotting for ProT α (acidic blotting). Samples obtained by boiling cultured cells for 5 min or samples of recombinant ProT α in Laemmli sample buffer were subjected to 15% SDS-PAGE fractionation and electrotransferred onto nitrocellulose membranes in acidic conditions in 20 mM sodium acetate buffer, pH 5.2, followed by fixation with 0.5% glutaraldehyde.¹⁴ The membranes were blocked with 5% non-fat milk in TBST (20 mM Tris-HCl, pH 7.6, 150 mM NaCl, 0.1% Tween-20) and probed with the antibody against ProT α (1 μ g/ml in 1% non-fat milk/TBST). Detection was performed using an HRP-conjugated goat anti-mouse IgG (Zymed Laboratories, San Francisco, CA, USA) and SuperSignal West Pico Chemiluminescent Substrate (PIERCE Biotechnology).

ATP measurement assay. Intracellular ATP was extracted from cells in the exponential phase of growth and measured by the luciferin/luciferase method using an ATP-Determination kit (Molecular Probes). Samples containing a total of 2×10^6 cells were subjected to the assay. Reaction buffer (200 μ l) containing 0.5 μ M luciferin, 1.25 μ g/ml luciferase, and 1 mM DTT was mixed with each cell lysate (20 μ l), and the luminescence was analyzed using a LUMAT LB 9507 luminometer (EG&G Berthold, Bad Wildbad, Germany).

Microinjection and time-lapse photography. C6 glioma cells were grown at a density of 2×10^5 cells/cm² on glass-bottom 35-mm dishes (Matsunami Glass Industries Ltd., Osaka, Japan) for 24 h at 37°C before use in experiments. The cells were imaged in Hanks buffer with or without serum. Microinjection was performed using an InjectMan NI2 microinjection system (Eppendorf AG, Hamburg, Germany). ProT α and BSA were conjugated to Alexa Fluor488 and with Alexa Fluor568 (Molecular Probes), respectively. Fluorescently labeled proteins (10 μ M in a needle) or ATP (3 mM in a needle) were injected into a cell at 45 hPa for 0.2 s. The injected fluorescently labeled proteins and fluorescent protein-fusion recombinants were imaged using an Axiovert 200 inverted microscope (Carl Zeiss) with a $\times 40$ Plan-Neofluar lens or a $\times 63$ Plan-Apochromat lens.

Fluorescence resonance energy transfer. C6 glioma cells expressing ProT α -EGFP and DsRed2-S100A13 were plated onto 96-well glass microplates and imaged in phenol red-free DMEM at 37°C. The fluorescence in each well was analyzed using a Fluostar Optima microplate reader (BMG Labtechnologies, Offenburg, Germany) with a 10-nm bandwidth excitation filter at 485 nm, and 10-nm bandwidth emission filters corresponding to 520 and 590 nm filters. The gain settings were identical for all experiments to maintain the relative contributions of the fluorescence to the detection channels contrast for spectral un-mixing. The 590/520-nm ratiometric images were acquired every 1 min for 120 min. The FRET efficiency was calculated as direct sensitization of the acceptor corresponding to acceptor fluorescence after excitation at 544 nm (acceptor photo-bleaching).

In vitro cleavage assay by caspase-3. Recombinant rat ProT α (1 μ g) was incubated with 10 μ g/ml recombinant active caspase-3 (Chemicon International Inc.) in the presence or absence of 10 μ M zDEVD-fmk (BD Biosciences, San Jose, CA, USA), a specific caspase group II inhibitor, in caspase buffer (20 mM PIPES pH 7.4, 100 mM NaCl, 1 mM EDTA, 0.1% CHAPS, 10% sucrose, and 10 mM DTT) for 1 h at 37°C.

Matrix-assisted laser desorption/ionization-time of flight. S100A13 was identified by using one-dimensional electrophoresis with in-gel digestion of bands followed by MALDI-TOF using an Ultraflex TOF/TOF system (Bruker Daltonics Inc., Billerica, MA, USA). Cleavage sites of rat ProT α by active caspase-3 were also identified by MALDI-TOF analysis. Detailed procedures have been described earlier.³⁴

Statistical analysis. All results are shown as means \pm S.E.M. Two independent groups were compared using the Student's *t*-test. Multiple groups

were compared using Dunnett's multiple comparison test after a one-factor ANOVA. $P < 0.05$ was considered significant.

Conflict of interest

The authors declare no conflict of interest.

Acknowledgements. We thank K Kidera, N Kiguchi, and N Takayama for technical assistance, and A Yoshida for valuable suggestions. We acknowledge Takeda Pharmaceutical Company Ltd., AB Vartapetian, and T. Maciag for providing amlexanox, the mouse anti-ProT α antibody, and the rabbit anti-S100A13 antibody. Parts of this study were supported by Grants-in-Aid for Scientific Research (to HU, B: 13470490 and B: 15390028) and Young Scientists (to HM, B: 20770105), on Priority Areas – Research on Pathomechanisms of Brain Disorders (to HU, 17025031, 18023028, 20023022) from the Ministry of Education, Culture, Sports, Science and Technology (MEXT), the Japan Society for the Promotion of Science (JSPS), and Health and Labour Sciences Research Grants on Research on Biological Resources and Animal Models for Drug Development (to HU, H20-Research on Biological Resources and Animal Models for Drug Development-003) from the Ministry of Health, Labour and Welfare.

1. Piñeiro A, Cordero OJ, Nogueira M. Fifteen years of prothymosin alpha: contradictory past and new horizons. *Peptides* 2000; **21**: 1433–1446.
2. Letsas KP, Frangou-Lazaridis M. Surfing on prothymosin alpha proliferation and anti-apoptotic properties. *Neoplasma* 2006; **53**: 92–96.
3. Gómez-Márquez J. Function of prothymosin alpha in chromatin decondensation and expression of thymosin beta-4 linked to angiogenesis and synaptic plasticity. *Ann N Y Acad Sci* 2007; **1112**: 201–209.
4. Jiang X, Kim HE, Shu H, Zhao Y, Zhang H, Kofron J *et al.* Distinctive roles of PHAP proteins and prothymosin-alpha in a death regulatory pathway. *Science* 2003; **299**: 223–226.
5. Ueda H, Fujita R, Yoshida A, Matsunaga H, Ueda M. Identification of prothymosin-alpha1, the necrosis-apoptosis switch molecule in cortical neuronal cultures. *J Cell Biol* 2007; **176**: 853–862.
6. Fujita R, Ueda H. Prothymosin-alpha1 prevents necrosis and apoptosis following stroke. *Cell Death Differ* 2007; **14**: 1839–1842.
7. Fujita R, Ueda M, Fujiwara K, Ueda H. Prothymosin-alpha plays a defensive role in retinal ischemia through necrosis and apoptosis inhibition. *Cell Death Differ* 2009; **16**: 349–358.
8. Prudovsky I, Mandinova A, Soldi R, Bagala C, Graziani I, Landriscina M *et al.* The non-classical export routes: FGF1 and IL-1alpha point the way. *J Cell Sci* 2003; **116**: 4871–4881.
9. Mouta Carreira C, LaVallee TM, Tarantini F, Jackson A, Lathrop JT, Hampton B *et al.* S100A13 is involved in the regulation of fibroblast growth factor-1 and p40 synaptotagmin-1 release *in vitro*. *J Biol Chem* 1998; **273**: 22224–22231.
10. Landriscina M, Soldi R, Bagala C, Micucci I, Bellum S, Tarantini F *et al.* S100A13 participates in the release of fibroblast growth factor 1 in response to heat shock *in vitro*. *J Biol Chem* 2001; **276**: 22544–22552.
11. Mandinova A, Soldi R, Graziani I, Bagala C, Bellum S, Landriscina M *et al.* S100A13 mediates the copper-dependent stress-induced release of IL-1alpha from both human U937 and murine NIH 3T3 cells. *J Cell Sci* 2003; **116**: 2687–2696.
12. Yasuda Y, Miyamoto Y, Saiwaki T, Yoneda Y. Mechanism of the stress-induced collapse of the Ran distribution. *Exp Cell Res* 2006; **312**: 512–520.
13. Shakulov VR, Vorobjev IA, Rubtsov YP, Chichkova NV, Vartapetian AB. Interaction of yeast importin alpha with the NLS of prothymosin alpha is insufficient to trigger nuclear uptake of cargos. *Biochem Biophys Res Commun* 2000; **274**: 548–552.
14. Sukhacheva EA, Evstafieva AG, Fateeva TV, Shakulov VR, Efimova NA, Karapetian RN *et al.* Sensing prothymosin alpha origin, mutations and conformation with monoclonal antibodies. *J Immunol Methods* 2002; **266**: 185–196.
15. Heizmann CW, Fritz G, Schäfer BW. S100 proteins: structure, functions and pathology. *Front Biosci* 2002; **7**: d1356–d1368.
16. Zimmer DB, Wright Sadosky P, Weber DJ. Molecular mechanisms of S100-target protein interactions. *Microsc Res Tech* 2003; **60**: 552–559.
17. Imai FL, Nagata K, Yonezawa N, Nakano M, Tanokura M. Structure of calcium-bound human S100A13 at pH 7.5 at 1.8 Å resolution. *Acta Crystallogr Sect F Struct Biol Cryst Commun* 2008; **64**: 70–76.
18. Shishibori T, Oyama Y, Matsushita O, Yamashita K, Furuichi H, Okabe A *et al.* Three distinct anti-allergic drugs, amlexanox, cromolyn and tranilast, bind to S100A12 and S100A13 of the S100 protein family. *Biochem J* 1999; **338** (Part 3): 583–589.
19. Matsunaga H, Ueda H. Synergistic Ca²⁺ and Cu²⁺ requirements of the FGF1-S100A13 interaction measured by quartz crystal microbalance: an initial step in amlexanox-reversible non-classical release of FGF1. *Neurochem Int* 2008; **52**: 1076–1085.

20. Enkemann SA, Wang RH, Trumbore MW, Berger SL. Functional discontinuities in prothymosin alpha caused by caspase cleavage in apoptotic cells. *J Cell Physiol* 2000; **182**: 256–268.
21. Evstafieva AG, Belov GA, Rubtsov YP, Kalkum M, Joseph B, Chichkova NV *et al.* Apoptosis-related fragmentation, translocation, and properties of human prothymosin alpha. *Exp Cell Res* 2003; **284**: 211–223.
22. Karetsov Z, Martic G, Tavoulari S, Christoforidis S, Wilm M, Gruss C *et al.* Prothymosin alpha associates with the oncoprotein SET and is involved in chromatin decondensation. *FEBS Lett* 2004; **577**: 496–500.
23. Subramanian C, Hasan S, Rowe M, Hottiger M, Orre R, Robertson ES. Epstein-Barr virus nuclear antigen 3C and prothymosin alpha interact with the p300 transcriptional coactivator at the CH1 and CH3/HAT domains and cooperate in regulation of transcription and histone acetylation. *J Virol* 2002; **76**: 4699–4708.
24. Karetsov Z, Kretsovali A, Murphy C, Tsolas O, Papamarcaki T. Prothymosin alpha interacts with the CREB-binding protein and potentiates transcription. *EMBO Rep* 2002; **3**: 361–366.
25. Martini PG, Katzenellenbogen BS. Modulation of estrogen receptor activity by selective coregulators. *J Steroid Biochem Mol Biol* 2003; **85**: 117–122.
26. Karapetian RN, Evstafieva AG, Abaeva IS, Chichkova NV, Filonov GS, Rubtsov YP *et al.* Nuclear oncoprotein prothymosin alpha is a partner of Keap1: implications for expression of oxidative stress-protecting genes. *Mol Cell Biol* 2005; **25**: 1089–1099.
27. Ueda H, Fujita R. Cell death mode switch from necrosis to apoptosis in brain. *Biol Pharm Bull* 2004; **27**: 950–955.
28. Ueda H. Prothymosin alpha plays a key role in cell death mode-switch, a new concept for neuroprotective mechanisms in stroke. *Naunyn Schmiedebergs Arch Pharmacol* 2008; **377**: 315–323.
29. Ueda H. Prothymosin alpha and cell death mode switch, a novel target for the prevention of cerebral ischemia-induced damage. *Pharmacol Ther* 2009; **123**: 323–333.
30. Jahn R, Scheller RH. SNAREs—engines for membrane fusion. *Nat Rev Mol Cell Biol* 2006; **7**: 631–643.
31. Martens S, McMahon HT. Mechanisms of membrane fusion: disparate players and common principles. *Nat Rev Mol Cell Biol* 2008; **9**: 543–556.
32. Nickel W. The mystery of nonclassical protein secretion. A current view on cargo proteins and potential export routes. *Eur J Biochem* 2003; **270**: 2109–2119.
33. Nickel W, Rabouille C. Mechanisms of regulated unconventional protein secretion. *Nat Rev Mol Cell Biol* 2009; **10**: 148–155.
34. Matsunaga H, Ueda H. Evidence for serum-deprivation-induced co-release of FGF-1 and S100A13 from astrocytes. *Neurochem Int* 2006; **49**: 294–303.
35. Matsunaga H, Ueda H. Voltage-dependent N-type Ca²⁺ channel activity regulates the interaction between FGF-1 and S100A13 for stress-induced non-vesicular release. *Cell Mol Neurobiol* 2006; **26**: 237–246.
36. Chichkova NV, Evstafieva AG, Lyakhov IG, Tsvetkov AS, Smirnova TA, Karapetian RN *et al.* Divalent metal cation binding properties of human prothymosin alpha. *Eur J Biochem* 2000; **267**: 4745–4752.
37. Fujita R, Ueda H. Protein kinase C-mediated necrosis-apoptosis switch of cortical neurons by conditioned medium factors secreted under the serum-free stress. *Cell Death Differ* 2003; **10**: 782–790.
38. Decker P, Muller S. Modulating poly (ADP-ribose) polymerase activity: potential for the prevention and therapy of pathogenic situations involving DNA damage and oxidative stress. *Curr Pharm Biotechnol* 2002; **3**: 275–283.
39. Lotze MT, Tracey KJ. High-mobility group box 1 protein (HMGB1): nuclear weapon in the immune arsenal. *Nat Rev Immunol* 2005; **5**: 331–342.
40. Harris HE, Raucci A. Alarmin(g) news about danger: workshop on innate danger signals and HMGB1. *EMBO Rep* 2006; **7**: 774–778.
41. Sburlati AR, Manrow RE, Berger SL. Human prothymosin alpha: purification of a highly acidic nuclear protein by means of a phenol extraction. *Protein Expr Purif* 1990; **1**: 184–190.
42. Fujita R, Ueda H. Protein kinase C-mediated cell death mode switch induced by high glucose. *Cell Death Differ* 2003; **10**: 1336–1347.

Supplementary Information accompanies the paper on Cell Death and Differentiation website (<http://www.nature.com/cdd>)